Biosensors and Bioelectronics 130 (2019) 307–314

Contents lists available at ScienceDirect

Biosensors and Bioelectronics

journal homepage: www.elsevier.com/locate/bios

Highly sensitive amperometric detection of glutamate by glutamic oxidase immobilized Pt nanoparticle decorated multiwalled carbon nanotubes (MWCNTs)/polypyrrole composite

Debasis Maity[a], R.T. Rajendra Kumar[a,b,*]

[a] DRDO - BU Center for Life Sciences, Bharathiar University, Coimbatore 641046, India
[b] Advanced Materials and Devices Laboratory (AMDL), Department of Nanoscience and Technology, Bharathiar University, Coimbatore 641046, Tamil Nadu, India

ARTICLE INFO

Keywords:
L-glutamate
Biosensor
Amperometric
PtNP
MWCNTs
Polypyrrole

ABSTRACT

A highly sensitive and selective glutamate biosensor using glutamate Oxidase (GlUtOx) immobilized platinum nanoparticle (PtNP) decorated multiwall carbon nanotube (MWCNTs)/polypyrrole (PPy) composite on glassy carbon electrodes (GC) is demonstrated. PtNP decorated MWCNTs (Pt-MWCNTs), PPy and Pt-MWCNTs/PPy composite were characterized by Field Emission Scanning Electron Microscope (FESEM), X-ray diffraction (XRD) and Raman analysis to confirm the formation of the nanocomposite. The glutamate Oxidase (GlUtOx) was immobilized on a GC/Pt-MWCNTs/PPy and characterized by the cyclic voltammetry (CV) and impedance spectroscopy (EIS) analysis. The fabricated L-glutamate biosensor exhibited high sensitivity (723.08 μA cm^{-2} mM^{-1}) with less response time (3 s) with a detection limit of 0.88 μM. The dynamic range from 10 to 100 μM with a correlation coefficient (R2) of 0.985 was observed for the L-glutamate biosensor. The analytical recovery of added L-glutamate acid (50 and 100 μM) in human serum soup were 96.1% and 97.5% respectively. The enzyme immobilized GC/Pt-MWCNTs/PPy/GlUtOx bioelectrode lost 12.6% and 23.8% of its initial activity after 30 days when stored at − 20 °C and 4 °C respectively.

1. Introduction

L-glutamic is a neurotransmitter especially in the mammalian central nervous system (CNS), which plays a major role (both physiological and pathological processes) in a wide range of brain functions (Abbott et al., 2006; Danbolt, 2001; Leibowitz et al., 2012; Oldendorf and Szabo, 1976; Pardridge, 2005). A lower level of L-glutamate can cause neuronal damage like lathyrism amyotrophic lateral sclerosis and Alzheimer's disease (Garthwaite, 1991; McCabe and Horn, 1988; Ye and Sontheimer, 1999). Also, L-glutamate is a biomarker for the different disease such as myocardial, hepatic and cancer cell (Dutta et al., 2013; Greenamyre and Young, 1989; Shi et al., 2010; Uchida et al., 1991). L-Glutamate also occurs naturally in specially protein-rich foods such as meat, fish, cheese, milk, mushrooms, and many vegetables (Goldschmiedt et al., 1990; Ito et al., 2017; Kazmi et al., 2017; Krishna Veni et al., 2010; Prescott, 2004; Rogers and Blundell, 1990) Under normal circumstances, L-glutamate level in the extracellular brain tissue and blood was in the range of 50–350 μM and 150–350 μM respectively (Leibowitz et al., 2012). So far, different methods such as chromatographic, spectrophotometric, capillary electrophoresis techniques, optical, potentiometric, chromatographic techniques, liquid chromatographic, titration and fluorimeters have been adopted to the determination of L-glutamate (Cordek et al., 1999; Eastwood et al., 2009; Hancu, 2009; Okumoto et al., 2005; Song et al., 2015; Spreux-Varoquaux et al., 2002) However, traditional methods require costly equipment, time-consuming sample preparation, and skilled persons to operate. On the other hand, electrochemical biosensing methods must overcome above drawbacks, as these are selective, sensitive, rapid, specific and quick (Liang et al., 2015; Yu et al., 2018).

Non-enzymatic biosensors were developed for the detection of L-glutamate using different electrode materials (Jamal et al., 2018, 2013). However, it was noticed that non-enzymatic biosensors had poor selectivity for the detection of the low level of L-glutamate (μM) (not suitable for field applications). The immobilization of glutamate oxidase on different nanomaterials modifications was proposed for the amperometric sensing of L-glutamate. (Amine et al., 2006; Batra and Pundir, 2013; Jamal et al., 2010; Özel et al., 2014). However, there are few issues such as low sensitivity and poor charge transfer rate from

* Corresponding author at: Advanced Materials and Devices Laboratory (AMDL), Department of Nanoscience and Technology, Bharathiar University, Coimbatore 641046, Tamil Nadu, India.
E-mail address: rtrkumar@buc.edu.in (R.T.R. Kumar).

https://doi.org/10.1016/j.bios.2019.02.001
Received 31 August 2018; Received in revised form 20 January 2019; Accepted 3 February 2019
Available online 04 February 2019
0956-5663/

analytic to the electrode and high working electrode potential, which need to be improved further to fabricate high-performance biosensor. Researchers have been working for decades to improve the sensitivity of glutamate sensor (Ammam and Fransaer, 2010; Gholizadeh et al., 2012). On the other hand, the different nanomaterials modified electrodes have opened a new possibility for the fabrication of high electrochemical activity and sensitive biosensors

The carbon-based nanomaterials (Carbon nanotubes (CNT), reduced graphene oxide (rGO)), metal nanoparticles (Ag, Au, Pt), conducting polymers (PPy, Polyaniline (PANI)) have been used to improve the analytic response of glutamate biosensors (Amine et al., 2006; Ammam and Fransaer, 2010; Jamal et al., 2010; Lei et al., 2014; Soldatkina et al., 2017). Nevertheless, high sensitivity, lower detection limit and selectivity towards L-glutamate in real-sample remains elusive, which need to be investigated further.

PPy was used for detection of l-glutamate due to its film-forming ability, good adhesion, nontoxicity, highly conductive, susceptible to chemical modification of sensors and improves the bonding between bioelectrodes and enzyme. (Wang and Musameh, 2005). PPy work as a conductive binder to improve the bonding formation between electrode and enzyme. It improves the signal and reduce chances of leaching during repeated measurement (Batra et al., 2016). PPy work was permselective layer for H_2O_2 in bioelectrode. The PPy and CNT composites commonly had been used to construct a robust biosensor with enhanced electrocatalytic activity compared to pure PPy. MWCNTs gives high surface area conducting network allows simple functionalization with PPy through π-π electrostatic interactions. PPy/MWCNTs/GlUtOx had been used for the detection of L-Glutamate (Ammam and Fransaer, 2010), however, this sensor had some disadvantages due to their low sensitivity. The PtNP most frequently used a catalyst in a variety of applications and possesses the best catalytic activity properties among all other pure metals NPs (Kim et al., 2012). Pt nanoparticles bonded to the sidewall of MWCNTs (Pt-MWCNTs) has proposed for the fabrication of novel chemical and biological sensors. The PtNP was used to modify MWCNTs, since it has the capability to improve the electrode conductivity also facilitate the electron transfer rate, thus improving the analytical selectivity and sensitivity.

In this work, we present on GlUtOx immobilized PtNP modified multiwalled CNTs and Polypyrrole nanocomposite coated glassy carbon electrode (GC/Pt-MWCNTs/PPy/GlUtOx) for highly sensitive and selective detection of L-glutamate. The fabrication and immobilization process was accomplished by simple drop casting method that allows for large-scale fabrication of sensor in less time compared to other reported methods. According to our knowledge, this is the first report on GC/Pt-MWCNTs/PPy/GlUtOx biosensor for the detection of L-glutamate. The sensitivity is extremely high (723.08 μA cm^{-2} mM^{-1}) that is nearly 3 time times higher than the previously reported highly sensitive L-glutamate sensors (Batra and Pundir, 2013). The other sensing parameters such as linear rage (10–100 μM), regression coefficient (R^2 = 0.985), response time (3 s), detection limit (0.88 μM), storage ability (30 days), reproducibility, performance against interference and real sample (serum) analysis are elucidated in detail.

2. Materials and methods

2.1. Reagents and Instrumentation

Sodium borohydride ($NaBH_4$), Potassium tetrachloroplatinate (K_2PtCl_4), Pyrrole, Iron(III) chloride ($FeCl_3$), Dopamine hydrochloride (DA), Ascorbic acid (AA), Uric acid (UA), Human Serum, L-glutamate, L-Glutamate Oxidase from *Streptomyces* species were purchased from Sigma Aldrich (analytical-grade). Ultrapure water (18.2 MU) was used throughout the experiment.

2.2. Apparatus used

Cyclic Voltammetric (CV), impedance spectroscopy (EIS) analysis and Amperometric measurements were performed (PARSTAT Multichannel; Model: PMC CHS08A) with three electrodes configuration. Where Pt wire work as an auxiliary electrode, Ag/AgCl electrodes were used as a reference electrode and GC/Pt-MWCNTs/PPy/GlUtOx used as a working electrode. Field emission electron microscope (FESEM). X-ray diffractometer (XRD) (X'pert Pro diffractometer), Raman analysis (Horiba Jobin Yvon) were used to analyze the sample.

2.3. Synthesis of GC/Pt-MWCNTs/PPy/GlUtOx bioelectrode

2.3.1. Synthesis of Pt-MWCNTs

Multiwall carbon nanotubes (MWCNTs) was synthesized by one step pyrolysis method using Ferrocene and Xylene as precursors at 870 °C (Maity et al., 2018). The uniform dispersion of MWCNTs with desired concentration (1 mg/ml) was made by probe sonication with 10 s on/off pulse. In a typical process, 0.2 ml of $K_2P_tCl_4$ (0.01 M) aqueous solution was added in 50 ml of as prepared MWCNTs solution assisted with mild sonication for 5 min. Followed by, 0.2 ml of $NaBH_4$ (0.1 M) was injected in K_2PtCl_4 contained MWCNTs solution to obtain Pt-MWCNTs with stirring at room temperature for 20 min. The resultant product was centrifuged and dispersed in millipore water and vacuum dried at 60 °C for overnight to obtain Pt-MWCNTs powder.

2.3.2. Synthesis of polypyrrole (PPy)

Polypyrrole was synthesized by in situ polymerization process. Pyrrole monomer (10 ml) was mixed with 50 ml water solution and it was stirred for 10 min at 4 °C to get a uniform dispersion. 20 ml of ferric chloride solution (0.1 M) was added drop by drop using pipette in pyrrole solution. The reaction was continued for 4 h under the same condition. The uniform deep blue colour polypyrrole was filtered with Buchner funnel and washed three times to remove unreacted monomer and oxidant.

2.3.3. Construction of GC/Pt-MWCNTs/PPy/GlUtOx bioelectrodes

Pt-MWCNTs/PPy nanocomposite was prepared by mixing Pt-MWCNTs and PPy (1:1) ratio in Millipore water followed by sonication for 30 min. Pt-MWCNTs/PPy solution (1 mg/ml) was drop cast (5 μL) using a micropipette on cleaned glassy carbon electrode and dried for 6 h at 60 °C. Glutamic oxidase stock solution (1 Unit in 100 μL) was prepared in phosphate buffer solution (0.1 M, pH 7.4) and kept at −20 °C until further usage. The prepared glutamic oxidase stock solution was carefully dropped cast (5 μL) an on Pt-MWCNTs/PPy coated GC and kept at 4 °C room temperature for overnight for the immobilization process. Next, the bioelectrode was shifted to a deep freezer (−20 °C) until usage to avoid degradation of the enzyme. The prepared glutamic oxidase immobilized GC/Pt-MWCNTs/PPy/GlUtOx electrodes were washed with double distilled water to remove the unbound enzyme from the surface of the electrode. The fabrication of bioelectrode is explained in the schematic as shown in Fig. 1.

2.4. Characterization of glutamate biosensor

The Cyclic voltammograms of GC/Pt-MWCNTs/PPy/GlUtOx was carried out using a galvanostat from 0.8 V to −0.6 V vs Ag/AgCl as reference electrode in the presence of phosphate buffer (20 ml) solution (0.1 M, pH-7.4) containing 5 mM $K_3Fe(CN)_6/K_4Fe(CN)_6$ with a scan rate from 10 to 100 mV/s. Electrochemical impedance spectroscopy (EIS) was used to measure the same platform in a frequency range from 500 kHz to 0.05 Hz. The electrode response was evaluated by using amperometric mode at 0.5 V Ag/AgCl by the addition of 200 μL of L-glutamate at room temperature (20 °C) in 20 ml phosphate buffer solution (0.1 M, pH-7.4).

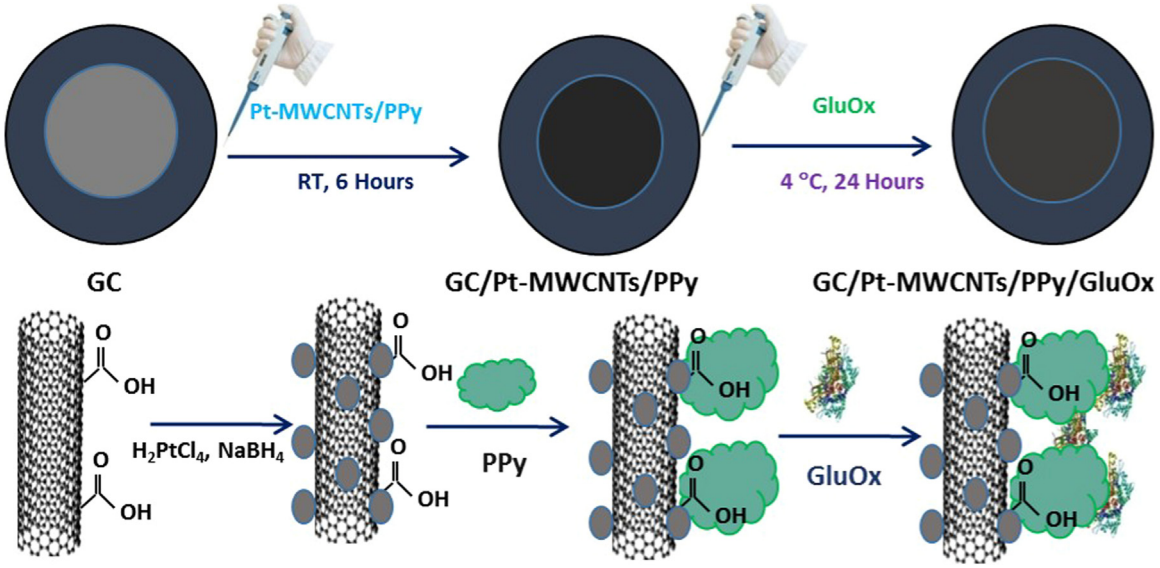

Fig. 1. Schematic explanation of GC/Pt-MWCNTs/PPy/GlUtOx modified glassy carbon electrode for glutamate biosensor.

2.5. Storage stability of GC/Pt-MWCNTs/PPy/GlUtOx electrode

The testing was performed at next day of immobilization process and during measurement, it was stored in a phosphate buffer solution. The bio-electrode was kept at 4 °C and −20 °C to analyze the storage stability and its effect on the sensing performance. The storage capability was performed every ten days for a period of one month.

3. Results and discussion

3.1. Characterization of Pt-MWCNTs/PPy

The structure and morphology of as-prepared MWCNTs, Pt-MWCNTs, PPy and PPy/Pt-MWCNTs nanocomposites were investigated by FESEM. MWCNTs showed randomly entangled and smooth surface morphology. MWCNTs with various diameter 50–100 nm and length 10–2 μm could observe (Fig. 2(a)) (Maity and Kumar, 2018). PtNP with the diameter range of 20–50 nm could be observed on the surface of MWCNTs (Fig. 2(b)). Fig. 2(c) shows disordered irregular particles and granular like morphology of PPy with an average size of 100–200 nm. As can be seen from Fig. 4(d) that Pt-MWCNTs and PPy composite have been homogeneously distributed. The large and higher magnification of above nanomaterial was provided in Supplementary information Fig. S1. X-ray diffraction(XRD) pattern and Raman spectra of MWCNTs, Pt-MWCNTs, PPy and PPY/Pt-MWCNTs were provided in Supplementary information Fig. S2. The further, EDX colour mapping present of different element and colour mapping of MWCNTs, Pt-MWCNTs, PPy and PPy/Pt-MWCNTs nanocomposites also provided in Supplementary information FigS3-S6.

3.2. Electrochemical characterizations

The electrochemical characterization of a modified glassy carbon electrode in the existence of external redox probe $[Fe(CN)^6]^{-3/-4}$ was investigated using cyclic voltammetry (CV) and electrochemical impedance spectroscopy (EIS). The glassy carbon electrode shows the redox behavior in the phosphate buffer solution containing 5 mM $[Fe(CN)^6]^{-3/-4}$ with a peak separation (ΔEp) of 0.923 V and a peak current (Ip) of 38.8 μA Fig. 3(a) and (b)). The peak current (Ip) for the MWCNTs and PPy modified electrode increased to 145 μA and 157 μA with peak separation (ΔEp) of 0.127 V and 0.163 V respectively (Fig. 3(b)). This might be because of MWCNTs and PPy that facilitate the electron transfer rate. Further, the peak current was increased to 391 μA and 562 μA for Pt-MWCNTs and Pt-MWCNTs/PPy modified glassy carbon electrode with peak separation (ΔEp) of 0.23 V and 0.41 V respectively. However, the peak current reduced to 456 μA in the presence of immobilized GlUtOx on Pt-MWCNTs/PPy modified glassy carbon electrode in the presence of 5 mM $[Fe(CN)^6]^{-3/-4}$ in phosphate buffer solution (pH 7.4, 0.1 M) at 100 mV/S scan rate. The insulating nature of GlUtOx might be because of a decrease in the charge transfer rate. Therefore, the fabricated highly electrocatalytic effect of GC/Pt-MWCNTs/PPy/GlUtOx bioelectrode was used for L-glutamate detection.Cyclic voltammetry (CV) of GC/Pt-MWCNTs/PPy/GlUtOx electrode at different scan rate (50–500 mV/s) in 5 mM $[Fe(CN)^6]^{-3/-4}$ in phosphate buffer solution (pH 7.4, 0.1 M), the calibration of I_{pa} and I_{pc} vs. square root of different scan rate and peak potentials vs logarithmic scan rates linear fit was provided in Supplementary information Fig. S7.

The electrochemical impedance spectroscopy (EIS) can give valuable information on the interface property of modified glassy carbon electrodes. Therefore, interfacial charge transfers characteristic of modified electrodes in each step were studied using an EIS curve as shown in Fig. 3(c and d). The semicircles diameter magnitude stands for the charge transfer resistance (R_{ct}) corresponding to faradaic resistance which was estimated from the equivalent circuit of the EIS curve (Fig. S8). The glassy carbon electrodes are shown higher R_{ct} value of 1000 Ω upon redox of 5 mM $[Fe(CN)^6]^{-3/-4}$ due to the extremely small electron transfer rate of GC. The R_{ct} value of MWCNTs and PPy modified electrode was 300 Ω and 500 Ω respectively.

This indicated that charge transfer rate was increased due to the high surface area of MWCNTs and PPy that facilitates the electron transfer. Further Pt-MWCNTs and Pt-MWCNTs/PPy modified GC have excellent conductive performance, which was indicated by lower R_{ct} value 60 Ω and 30 Ω respectively. Therefore, GC/Pt-MWCNTs/PPy electrode has good electron pathways between solution and electrode for excellent electrochemical sensing platform. Upon the immobilization of glutamic oxidase on GC/Pt-MWCNTs/PPy electrode, the R_{ct} value increased to 154 Ω (Fig. S8). This can be attributed to the poor electrical conductivity of the enzyme, which hinders the electrons transfer. This result confirms the successful immobilization of enzymes on GC/Pt-MWCNTs/PPy electrode surface.

3.3. Optimization of pH and working potential

An optimum pH range for L-glutamate sensing is important to study as it influences the electrochemical behavior and bioactivity of the enzyme. The effect of pH on the bioelectrode response was investigated

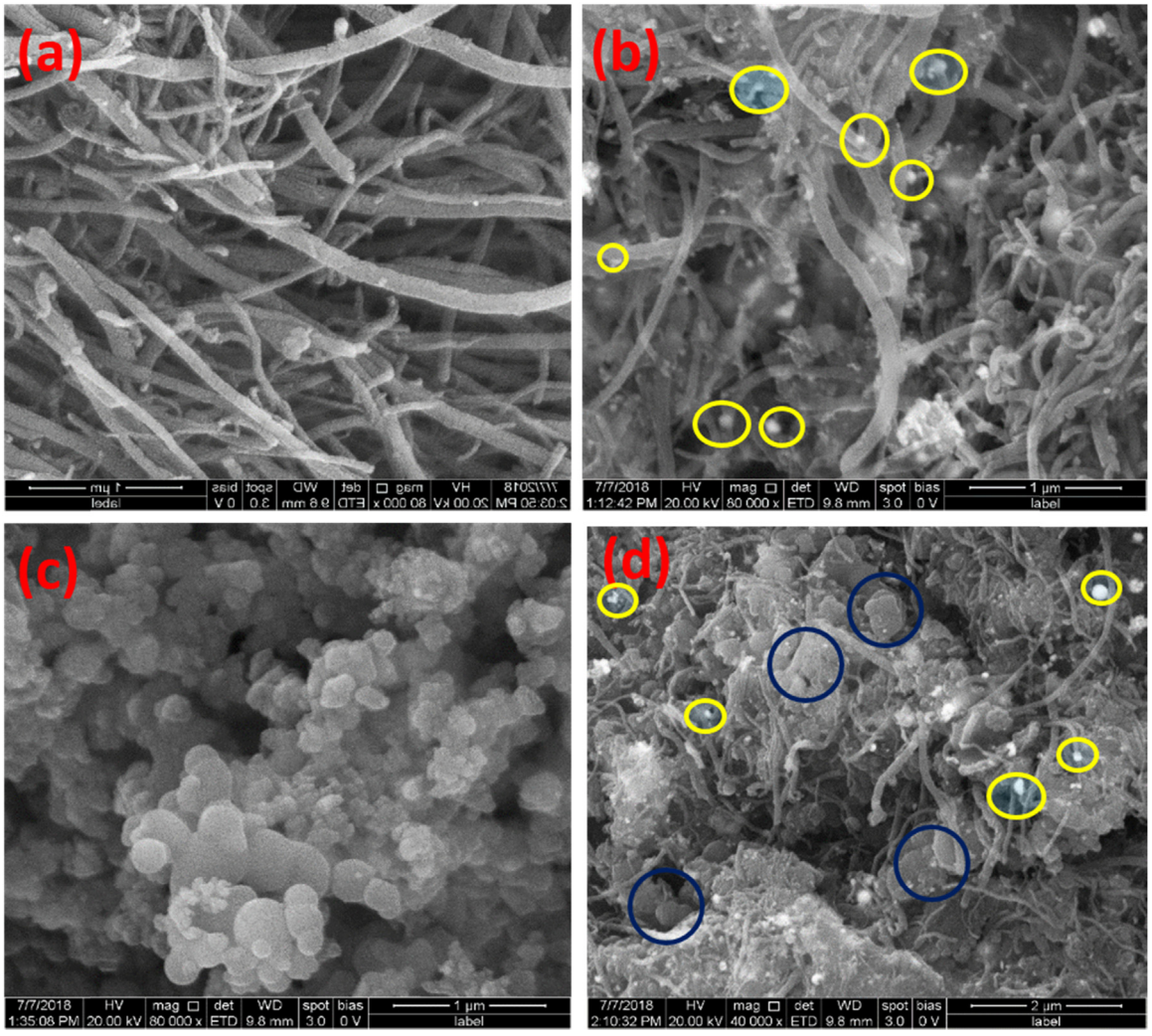

Fig. 2. FESEM image of (a) MWCNTs (b) Pt decorated MWCNTs (c) PPy (d) Pt-MWCNTs/PPy.

in the range pH 5.0–9.0 by the addition of L-glutamate (10 μM) (Fig. 4(a)). It can be noticed that the electrochemical response of the GC/Pt-MWCNTs/PPy/GlUtOx electrode was poor when it was in the strongly acidic and alkaline environment. The high acidity leads to decrease the GlUtOx activity, where alkalinity medium causes a decrease in GlUtOx activity too. The optimum current was obtained for GC + Pt-MWCNTs/PPy/GlUtOx electrode at pH 7.4 and it was selected for the subsequent experiments for L-glutamate sensing.

From Fig. 4(b), it can be seen that the L-glutamate biosensor response found to be increased gradually up to 0.5 V and increase slowly up to the measurement of the voltage of 0.70 V by the addition of L-glutamate (10 μM). Therefore, subsequent studies were carried out at 0.5 V to get an optimum response with low interference signal. The experiments were carried out at the optimum temperature of 30 °C to avoid thermal inactivity of the enzyme. Therefore, amperometric response of GC/Pt-MWCNTs/PPy/GlUtOx was carried out in phosphate buffer solution (pH 7.4, 0.1 M) by the addition of 100 μL L-glutamate at applied voltage 0.5 V.

Cyclic Voltammetric (CV) response of GC/Pt-MWCNTs/PPy/GlUtOx in phosphate buffer solution was shown with different concentration of L-glutamate in Supplementary information Fig. S9. It was observed that no oxidation and reduction of bioelectrode was found in the absence of L-glutamate. CV studies demonstrate the enzymatical reaction in the presence of L-glutamate shown as an increase in the current and the maxima obtained at 0.5 V due to the production of H_2O_2.

The electrochemical response of biosensor can be described by the following equations.

$$L - glutamate + O_2 \xrightarrow[Glutamic\ Oxidase]{} 2-\text{oxoglutarate} + NH_3 + H_2O_2 \quad (1)$$

$$H_2O_2 \rightarrow 2H^+ + O_2 + 2e^- \quad (2)$$

Eq. (1) represents the enzymatic oxidation process of the L-glutamate to form 2-oxoglutarate and H_2O_2. Eq. (2) describes the electrochemical detection of H_2O_2 at the base transducer, which generates the analytical signal during measurement of L-glutamate.

3.4. Amperometric determination of L-glutamate

3.4.1. Evaluation of biosensor

The amperometric technique was further used for the determination of L-glutamate using GC/Pt-MWCNTs/PPy/GlUtOx modified electrode. Fig. 5(a) shows the characteristic amperometric (i-t) response of GC/Pt-MWCNTs/PPy/GlUtOx bio-electrode to the addition of 10 μM L-glutamate into the 0.1 M phosphate buffer solution at applied potential 0.5 V. It was observed that the addition of 10 μM L-glutamate in each time produced a stable and well-defined amperometric response. The response was found to be increased with L-glutamate concentration from 10 to 100 μM. The GC/Pt-MWCNTs/ GlUtOx and GC/MWCNTs/ GlUtOx biosensor was also investigated under addition of L-glutamate to understand the role of PPy and PtNP on sensing performance (Fig. S10 and 11). It was found that PPy work as a conductive binder to

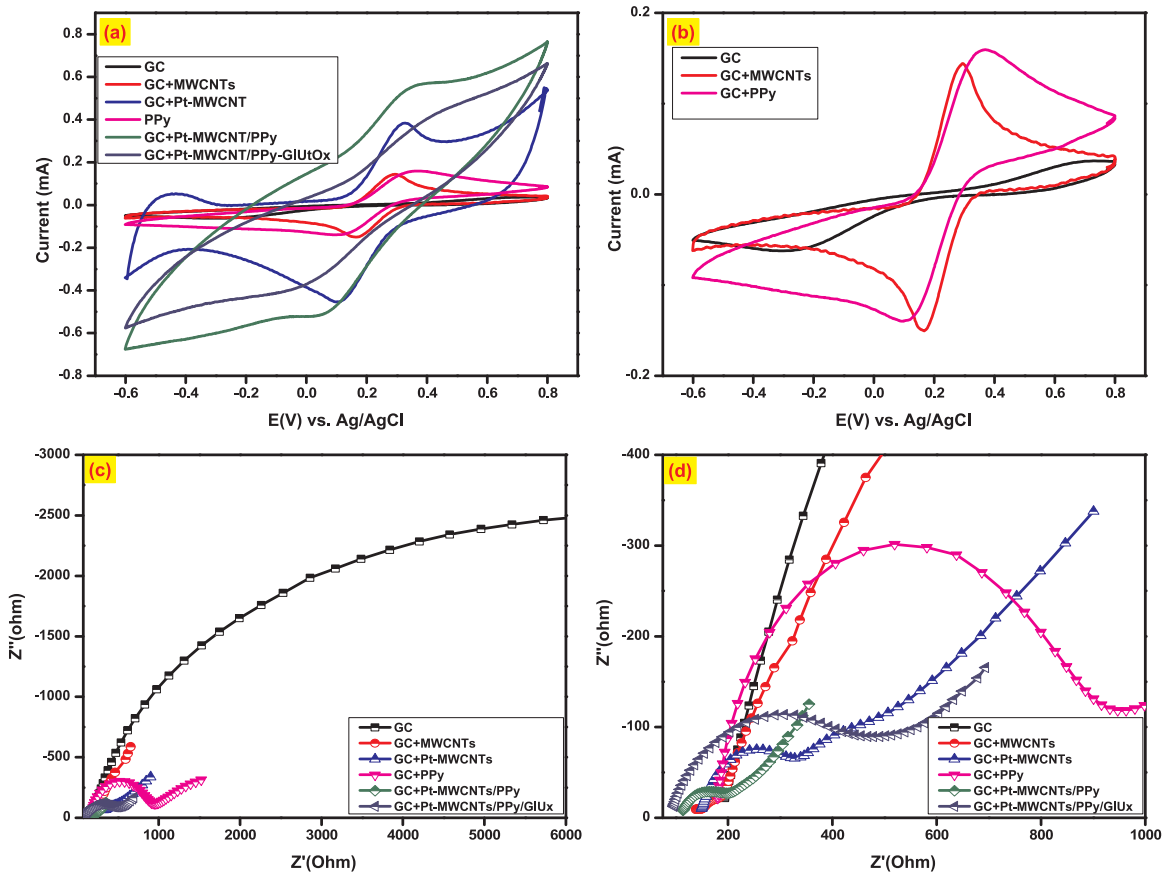

Fig. 3. (a) and (b) Cyclic voltammetry (CV), (c) and (d) electrochemical impedance spectroscopy (EIS) of modified electrodes at different stages in 5 mM $[Fe(CN)^6]^{-3/-4}$ in phosphate buffer solution (pH 7.4, 0.1 M).

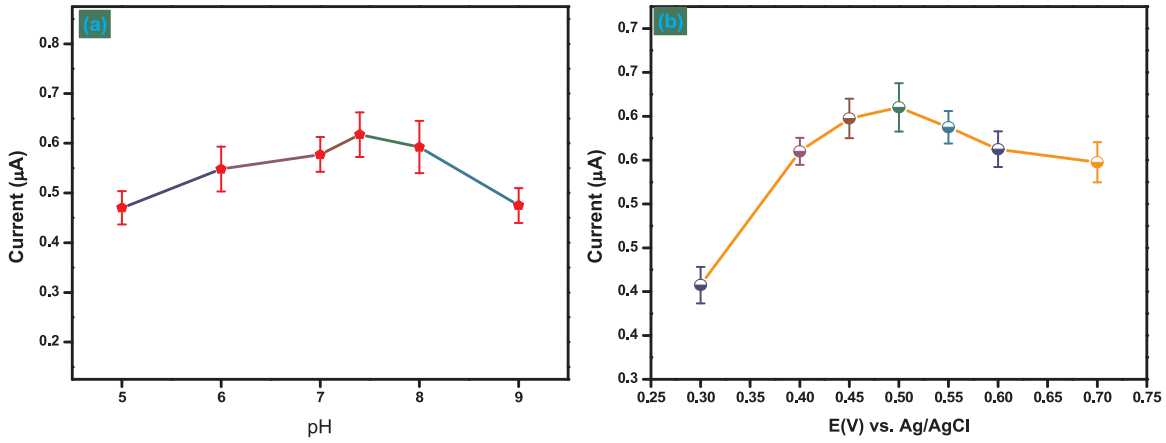

Fig. 4. Optimization of the modified GC/Pt-MWCNTs/PPy/GlUtOx on the effect of (a) pH of buffer solution (b) operating potential by the addition of L-glutamate (10 μM).

improve the bonding formation between electrode and enzyme. Therefore, it leads to improvement in the single and remoted chances of leaching during repeated measurement (Batra et al., 2016).

3.4.2. Linearity and Detection limit

Fig. 5(b) shows the calibration of current response against L-glutamate concentration range from 10 μM to 100 μM. The linear regression equation I (μA) = 0.05*x + 0.065 (μA) (c); R^2 = 0.9853 was fitted with L-glutamate concentration. The sensitivity of GC/Pt-MWCNTs/PPy/GlUtOx biosensor sensor was calculated as high as 723.08 μA cm^{-2} mM^{-1}. The calculated limit of detection (LOD) was 0.88 μM for S/N = 3.

The enzyme substrate was calculated by using Lineweaver- Burk equation

$$\frac{1}{I} = \left(\frac{K_M^{app}}{I_{max}} \times \frac{1}{C}\right) + \frac{1}{I_{max}}. \quad (3)$$

where K_M^{app}, C, I_{max} and I were Michaelis–Menten constant, L-glutamate concentration, saturated current and measured current respectively. The calculated value for Lineweaver–Burk plot of K_M^{app} for L-glutamate biosensor was 3.6 × 10^{-4} /μMμA (Fig. S12). The lower value of K_M^{app} indicates that the GC/Pt-MWCNTs/PPy/GlUtOx bioelectrode based biosensor exhibits a higher affinity to L-glutamate oxidase for the detection of L-glutamate (Ahmad et al., 2014).

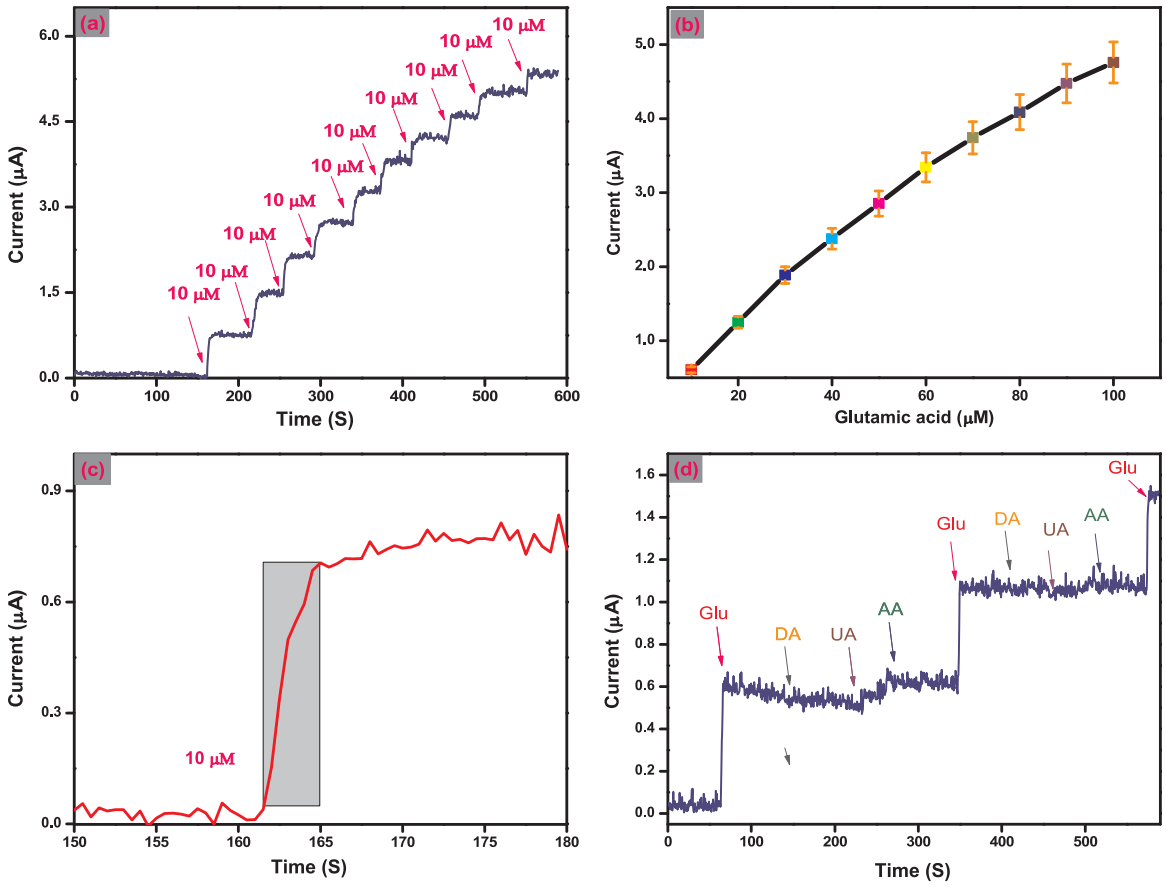

Fig. 5. (a) An amperometric (i-t) response of GC/Pt-MWCNTs/PPy/GlUtOx bioelectrode upon the addition of 10 μM L-glutamate into 0.1 phosphate buffer solution at the applied potential of 0.5 V (b) The corresponding calibration for Current Vs L-glutamate concentration (c) The response times in addition of L-glutamate (d) In the same condition amperometric response of GC/Pt-MWCNTs/PPy/GlUtOx upon the addition of 10 μM with ascorbic acid (100 μM), dopamine (100 μM), uric acid (100 μM) and glucose (100 μM).

3.4.3. Response time

The response time of GC/Pt-MWCNTs/PPy/GlUtOx sensor for L-glutamate was calculated as 3 s (Fig. 5(c)). This shows that the biosensor has fasts electrocatalysis behavior towards L-glutamate at GC/Pt-MWCNTs/PPy/GlUtOx electrode surface.

3.4.4. Interference study of GC/Pt-MWCNTs/PPy/GlUtOx biosensor

The effect of the presence of interfering compounds such as ascorbic acid (AA), dopamine (DA), glucose (Glu), uric acid (UA) in presence of 10 μM L-glutamate (Glut) is shown in Fig. 5(d). These compounds are the major elements that affect the detection of L-glutamate in blood. It can be seen from Fig. 5(d) that these interference compounds have not affected the L-glutamate sensing process. The selective nature of glutamic oxidase and low working potential of composite electrodes avoids the sensing of interference compounds.

3.4.5. Comparable study of GC/Pt-MWCNTs/PPy/GlUtOx L-glutamate biosensor

The analytical performances of GC/Pt-MWCNTs/PPy/GlUtOx based L-glutamate biosensor (sensitivity, LOD, and applied potential) was compared with previously reported sensors in terms of sensitivity, LOD, applied potential using carbon nanotubes and other nanoparticles modified electrodes (Table 1).

From Table 1, it was confirmed that our fabricated GC/Pt-MWCNTs/PPy/GlUtOx based L-glutamate biosensor exhibits good performance in a different category. The sensor exhibits the highest sensitivity with a comparable linear range and LOD compared with another recently reported L-glutamate biosensor. The excellent analytical performance (such as sensitivity, LOD, wider linear response) of the Pt-MWCNTs/PPy/GlUtOx modified glassy carbon electrode may attribute for the following reasons, (a) The higher electrochemical performance of carbon-based nanostructure MWCNTs, (b) PtNP to enhance electrons transfer rate (c) conducting polymer PPy, which act as a conducting binder of nanocomposite and π–π stacking interaction between MWCNTs and PPy rings (d) selective interaction of enzyme (Glutamic oxidase) towards substrate (L-glutamate) resulting in a boosted electrocatalytic activity towards L-glutamate and enhanced electrochemical activity.

3.4.6. Analytical recovery

The analytical recovery experiment was done to explore the particle applications of GC/Pt-MWCNTs/PPy/GlUtOx fabricated biosensors. The GC/Pt-MWCNTs/PPy/GlUtOx biosensor was examined in 0.1 M phosphate buffer solution (pH 7.4, at +0.50 V) containing diluted four different concentrations of the human serum sample with known L-glutamate concentration. The average recoveries of L-glutamate added serum (50 and 100 μM) were 96.1% and 97.5% respectively demonstrating the satisfied reliability of the fabricated biosensor. (Table 2)

3.4.7. Stability, reproducibility and storage ability of enzyme electrode

The reproducibility of the electrode was verified by applying ten electrodes in 100 μM of L-glutamate for measurement. The relative standard deviation value was found at 12.7%. The electrodes response current was decreased by 9.47% after ten successive measurements. The biosensor was stored at two different temperatures over a period of one month. The GC/Pt-MWCNTs/PPy/GlUtOx bioelectrode performance was analyzed for once in ten days for one month, at the end of the month it maintained 76.2% (at 4 °C) and 87.4 % (at −20 °C) of its

Table 0.1
Comparison table of the analytical parameters obtained at GC/Pt-MWCNTs/PPy/GlUtOx with the previously reported L-glutamate sensor.

Modified electrode	Im	pH & Temp	Methods	E_{ap} (V)	Linear range (μM)	Sensitivity ($\mu A m M^{-1} cm^{-2}$)	LOD (μM)	Storage (Days)	Application	Reference
Pt/Nafion/GlUtOx	Cox	7.8,37 °C	A	0.6	0–500	0.325	0.6	–	–	(Pan and Arnold, 1996)
Graphite electrode/GlUtOx	Cox	–	A	–	1–125	0.129	0.7	–	–	(Ryan et al., 1997)
Polycarbamylsulfonate-hydrogel/GlUtOx	Ads	6.86, RT	A	0.4	100–5000	0.194	1.01	14	soy sauce	(Kwong et al., 2000)
Polycarbonate/GlUtOx	Cox	6.0, -	A	0.085	68–1271	0.009	68	5	Food	(Nakorn et al., 2003)
PPy/MWCNTs/GlUtOx	–	7.4,37 °C	A	0.65	0–140	10.76	0.3	14	–	(Ammam and Fransaer, 2010)
The GlUtOx/TGA/Au	Cox	7.4,-	CV	–	0.1–10000	20.75	0.089	30	–	(Rahman, 2011)
GlUtOx/eMWCNT/AuNP/CHIT	Ads	7.5, 37 °C	CV	0.135	5–500	155	1.6	7	Serum	(Batra and Pundir, 2013)
CeO2/TiO2/GlUtOx/Chit/o- PD/Pt	Ads	7.4,-	A	0.6	5–50	0.793	0.594	10	cerebrospinal fluid	(Özel et al., 2014)
GlUtOx/ZnO-NR/PPy/PGE	Ads	7.4, 30 °C	A	0.065	0.02–500	1.4	0.00018	80	Foodstuffs	(Batra et al., 2016)
Silicon-based MEA probe	Ads	7.4, 25 °C	A	0.7	5–109	204	1.68	30	serum	(Hoa et al., 2018)
GlUtOx/Pt DEN-functionalized SWCNT	Cox	7.4,-	CV	–	0.0001–100	–	0.0009	–	rice soups	(Lee et al., 2018)
Pt/ta-C/APTES/GlOx	Cox	6.2,4 °C	A	0.6	10–1000	2.9	10	49	–	(Kaivosoja et al., 2015)
Nafion/Gldh-bacteria/PEI-MWNTs/GCE	Ads	7.4, 25 °C	A	0.52	10–1000	–	2	15	chicken essence, soy sauce	(Liang et al., 2015)
PPy/nafion/CHIT/GlOx	Ads	–	A	0.7	10–887	38	2.5	9	–	(Tseng et al., 2013)
Polyimide substrate pt micro electrodes	Cox	7.4,32 °C	A	0.45	10–150	216	–	28	In vivo	(Weltin et al., 2014)
CHIT/GlutOx	Cox	7.4,-	A	0.7	20–217	34.9	6.5	–	In vivo	(Tseng et al., 2014)
GC/Pt-MWCNTs/PPy/GlUtOx	Ads	7.4, 30 °C	A	0.5	10–100	723.08	0.88	30	Serum	This work

* A- Amperometric, D- Dometric, Cox-Crosslinking, Ads- Adsorption, Im-Immobilization Methods, Temp-Temperature.

Table 2
Determination of L-glutamate in human serum samples.

Samples	Added L-glutamate (μM)	Found L-glutamate (μM)	Recovery (%)	RSD (n = 3) (%)
1	50	47.9	95.8	7.2
2	50	48.40	96.4	5.1
3	100	97.2	97.2	4.8
4	100	97.8	97.8	6.5

initial response.

These fabricated high-performance GC/Pt-MWCNTs/PPy/GlUtOx L-glutamate acid biosensor have excellent sensitivity, fast response, the lower detection limit for the detection of L-glutamate in practical samples like a human serum. The present method and material can be attributed to the immobilization of glutamic oxidase for commercial application to the detection of L-glutamate for various applications.

4. Conclusion

In this study, we construct a high-performance L-glutamate biosensor, in terms of sensitivity (723.08 μA cm^{-2} mM^{-1}), lowest detection limit (0.88 μM), good working range (10–100 μM), quicker response (3 s), and better storage stability (30 days) when compared to reported biosensors. The novel insights into Pt-MWCNTs/PPy nanocomposite could be used to enhance the analytical performance of other enzyme-based sensors. Additionally, the GC/Pt-MWCNTs/PPy/GlUtOx biosensor exhibited excellent anti-interference ability, long-term storage stability, repeatability and reproducibility for the fabrication of high-performance L-glutamate biosensor that is suitable for practical applications. Therefore, future research could also be focused on the fabrication of a cost-effective screen printed system enabled biosensor, which can be used in clinical studies for real-time and continuous monitoring of L-glutamate.

Acknowledgments

Dr. R. T. R gratefully acknowledges the financial support by the Defence Research and Development Organisation (DRDO), New Delhi, Govt of India (grant no. DLS/86/50011/DRDO-BU center/1748/D (R& D). The authors acknowledge, Dr. K. Kadirvelu, Joint Director,DRDO-BU Center for Life Science, Coimbatore and Dr. N. S. Kumar, Associate Director, Defence Bioengineering and Electromedical Laboratory (DEBEL),Bengalore for continuous support throughout the work.

Credit author statement

Ms. Debasis Maity involved in the design, execution of the work and wrote the first draft of the manuscript. Dr. R T Rajendra Kumar contributed on concept, interpretation and supervised the work.

Declaration of interests

The authors declare that they have no known competing financial interests or personal relationships that could have appeared to influence the work reported in this paper.

Appendix A. Supporting information

Supplementary data associated with this article can be found in the online version at doi:10.1016/j.bios.2019.02.001.

References

Abbott, N.J., Rönnbäck, L., Hansson, E., 2006. Nat. Rev. Neurosci. 7, 41–53. https://doi.org/10.1038/nrn1824.

Ahmad, R., Tripathy, N., Kim, S.H., Umar, A., Al-Hajry, A., Hahn, Y.B., 2014. Electrochem. Commun. 38, 4–7. https://doi.org/10.1016/j.elecom.2013.10.028.
Amine, A., Mohammadi, H., Bourais, I., Palleschi, G., 2006. Biosens. Bioelectron. 21, 1405–1423. https://doi.org/10.1016/j.bios.2005.07.012.
Ammam, M., Fransaer, J., 2010. Biosens. Bioelectron. 25, 1597–1602. https://doi.org/10.1016/j.bios.2009.11.020.
Batra, B., Pundir, C.S., 2013. Biosens. Bioelectron. 47, 496–501. https://doi.org/10.1016/j.bios.2013.03.063.
Batra, B., Yadav, M., Pundir, C.S., 2016. Biochem. Eng. J. 105, 428–436. https://doi.org/10.1016/j.bej.2015.10.012.
Cordek, J., Wang, X., Tan, W., 1999. Anal. Chem. 71, 1529–1533.
Danbolt, N.C., 2001. Glutamate uptake.1016/S0301-0082(00)00067-00068.
Dutta, S., Ray, S., Nagarajan, K., 2013. Saudi Pharm. J. 21, 337–343. https://doi.org/10.1016/j.jsps.2012.12.007.
Eastwood, K., Else, P., Charlett, A., Wilcox, M., 2009. J. Clin. Microbiol. 47, 3211–3217. https://doi.org/10.1128/JCM.01082-09.
Garthwaite, J., 1991. Trends Neurosci. 14, 60–67. https://doi.org/10.1016/0166-2236(91)90022-M.
Gholizadeh, A., Shahrokhian, S., Iraji zad, A., Mohajerzadeh, S., Vosoughi, M., Darbari, S., Sanaee, Z., 2012. Biosens. Bioelectron. 31, 110–115. https://doi.org/10.1016/j.bios.2011.10.002.
Goldschmiedt, M., Redfern, J.S., Feldman, M., 1990. Am. J. Clin. Nutr. 51, 794–797. https://doi.org/10.1093/ajcn/51.5.794.
Greenamyre, J.T., Young, A.B., 1989. Neurobiol. Aging 10, 593–602. https://doi.org/10.1016/0197-4580(89)90143-7.
Hancu, I., 2009. J. Magn. Reson. Imaging 30, 1155–1162. https://doi.org/10.1002/jmri.21936.
Hoa, L., Hoa, Q., Chen, H., Tseng, T.T., 2018. Electroanalysis 30, 561–570. https://doi.org/10.1002/elan.201700762.
Ito, H., Ueno, H., Kikuzaki, H., 2017. Integr. Food, Nutr. Metab. 4. https://doi.org/10.15761/IFNM.1000186.
Jamal, M., Chakrabarty, S., Shao, H., McNulty, D., Yousuf, M.A., Furukawa, H., Khosla, A., Razeeb, K.M., 2018. Technology 6, 1–7. https://doi.org/10.1007/s00542-018-3724-6.
Jamal, M., Hasan, M., Mathewson, A., Razeeb, K.M., 2013. Biosens. Bioelectron. 40, 213–218. https://doi.org/10.1016/j.bios.2012.07.024.
Jamal, M., Xu, J., Razeeb, K.M., 2010. Biosens. Bioelectron. 26, 1420–1424. https://doi.org/10.1016/j.bios.2010.07.071.
Kaivosoja, E., Tujunen, N., Jokinen, V., Protopopova, V., Heinilehto, S., Koskinen, J., Laurila, T., 2015. Talanta 141, 175–181. https://doi.org/10.1016/j.talanta.2015.04.007.
Kazmi, Z., Fatima, I., Perveen, S., Malik, S.S., 2017. Int. J. Food Prop. 20, 1807–1815. https://doi.org/10.1080/10942912.2017.1295260.
Kim, S.K., Kim, D., You, J.M., Han, H.S., Jeon, S., 2012. Electrochim. Acta 81, 31–36. https://doi.org/10.1016/j.electacta.2012.07.070.
Krishna Veni, N., Karthika, D., Surya Devi, M., Rubini, M.F., Vishalini, M., Pradeepa, Y.J., 2010. J. Young Pharm. 2, 297–300. https://doi.org/10.4103/0975-1483.66795.
Kwong, A.W.K., Gründig, B., Hu, J., Renneberg, R., 2000. Biotechnol. Lett. 22, 267–272. https://doi.org/10.1023/A:1005694704872.
Lee, C.S., Ju, Y., Kim, J., Kim, T.H., 2018. Sens. Actuators B Chem. 275, 367–372. https://doi.org/10.1016/j.snb.2018.08.030.
Lei, W., Si, W., Xu, Y., Gu, Z., Hao, Q., 2014. Microchim. Acta 181, 707–722. https://doi.org/10.1007/s00604-014-1160-6.
Leibowitz, A., Boyko, M., Shapira, Y., Zlotnik, A., 2012. Int. J. Mol. Sci. 13, 10041–10066. https://doi.org/10.3390/ijms130810041.
Liang, B., Zhang, S., Lang, Q., Song, J., Han, L., Liu, A., 2015. Anal. Chim. Acta 884, 83–89. https://doi.org/10.1016/j.aca.2015.05.012.
Maity, D., Rajavel, K., Kumar, R.T.R., 2018. Sens. Actuators B Chem. 261, 297–306. https://doi.org/10.1016/j.snb.2018.01.152.
Maity, D., Kumar, R.T.R., 2018. ACS Sens. 3, 1822–1830. https://doi.org/10.1021/acssensors.8b00589.
McCabe, B.J., Horn, G., 1988. Proc. Natl. Acad. Sci. USA 85, 2849–2853. 〈https://doi.org/10.1073/pnas.85.8.2849〉.
Nakorn, P.N., Suphantharika, M., Udomsopagit, S., Surareungchai, W., 2003. World J. Microbiol. Biotechnol. 19, 479–485. https://doi.org/10.1023/A:1025181317237.
Okumoto, S., Looger, L.L., Micheva, K.D., Reimer, R.J., Smith, S.J., Frommer, W.B., 2005. Proc. Natl. Acad. Sci. USA 102, 8740–8745. https://doi.org/10.1073/pnas.0503274102.
Oldendorf, W.H., Szabo, J., 1976. Am. J. Physiol. 230, 94–98.
Özel, R.E., Ispas, C., Ganesana, M., Leiter, J.C., Andreescu, S., 2014. Biosens. Bioelectron. 52, 397–402. https://doi.org/10.1016/j.bios.2013.08.054.
Pan, S., Arnold, M.A., 1996. Talanta 43, 1157–1162. https://doi.org/10.1016/0039-9140(95)01854-9.
Pardridge, W.M., 2005. NeuroRx 2, 3–14. https://doi.org/10.1602/neurorx.2.1.3.
Prescott, J., 2004. Appetite 42, 143–150. https://doi.org/10.1016/j.appet.2003.08.013.
Rahman, M.M., 2011. J. Biomed. Nanotechnol. 7, 351–357. https://doi.org/10.1166/jbn.2011.1299.
Rogers, P.J., Blundell, J.E., 1990. Physiol. Behav. 48, 801–804. https://doi.org/10.1016/0031-9384(90)90230-2.
Ryan, M.R., Lowry, J.P., O'Neill, R.D., 1997. Analyst 122, 1419–1424. https://doi.org/10.1039/a704508e.
Shi, Z., Luscombe-Marsh, N.D., Wittert, G.A., Yuan, B., Dai, Y., Pan, X., Taylor, A.W., 2010. Br. J. Nutr. 104, 457–463. https://doi.org/10.1017/S0007114510000760.
Soldatkina, O.V., Soldatkin, O.O., Kasap, B.O., Kucherenko, D.Y., Kucherenko, I.S., Kurc, B.A., Dzyadevych, S.V., 2017. Nanoscale Res. Lett. 12. https://doi.org/10.1186/s11671-017-2026-8.
Song, J., Liang, B., Han, D., Tang, X., Lang, Q., Feng, R., Han, L., Liu, A., 2015. Enzym. Microb. Technol. 70, 72–78. https://doi.org/10.1016/j.enzmictec.2014.12.002.
Spreux-Varoquaux, O., Bensimon, G., Lacomblez, L., Salachas, F., Pradat, P.F., Le Forestier, N., Marouan, A., Dib, M., Meininger, V., 2002. J. Neurol. Sci. 193, 73–78. https://doi.org/10.1016/S0022-510X(01)00661-X.
Tseng, T.T.C., Chang, C.F., Chan, W.C., 2014. Molecules 19, 7341–7355. https://doi.org/10.3390/molecules19067341.
Tseng, T.T.C., Yao, J., Chan, W.C., 2013. Biochem. Eng. J. 78, 146–153. https://doi.org/10.1016/j.bej.2013.04.019.
Uchida, Y., Takio, K., Titani, K., Ihara, Y., Tomonaga, M., 1991. Neuron 7, 337–347. https://doi.org/10.1016/0896-6273(91)90272-2.
Wang, J., Musameh, M., 2005. Acta 539, 209–213. https://doi.org/10.1016/j.aca.2005.02.059.
Weltin, A., Kieninger, J., Enderle, B., Gellner, A.K., Fritsch, B., Urban, G.A., 2014. Biosens. Bioelectron. 61, 192–199. https://doi.org/10.1016/j.bios.2014.05.014.
Ye, Z.C., Sontheimer, H., 1999. Cancer Res. 59, 4383–4391. https://doi.org/10.1016/0896-6273(88)90162-6.
Yu, L., Zhang, Q., Jin, D., Xu, Q., Hu, X., 2018. Talanta. https://doi.org/10.1016/j.talanta.2018.12.090.